SAR and QSAR in Environmental Research

ISSN: 1062-936X (Print) 1029-046X (Online) Journal homepage: https://www.tandfonline.com/loi/gsar20

Synthesis and investigation of binding interactions of 1,4-benzoxazine derivatives on topoisomerase IV in *Acinetobacter baumannii*

S. Yilmaz, I. Yalcin, S. Okten, F. K. Onurdag & E. Aki-Yalcin

To cite this article: S. Yilmaz, I. Yalcin, S. Okten, F. K. Onurdag & E. Aki-Yalcin (2017) Synthesis and investigation of binding interactions of 1,4-benzoxazine derivatives on topoisomerase IV in *Acinetobacter baumannii*, SAR and QSAR in Environmental Research, 28:11, 941-956, DOI: 10.1080/1062936X.2017.1404490

To link to this article: https://doi.org/10.1080/1062936X.2017.1404490

SAR AND QSAR IN ENVIRONMENTAL RESEARCH, 2017
VOL. 28, NO. 11, 941–956
https://doi.org/10.1080/1062936X.2017.1404490

Taylor & Francis
Taylor & Francis Group

Synthesis and investigation of binding interactions of 1,4-benzoxazine derivatives on topoisomerase IV in *Acinetobacter baumannii*[$]

S. Yilmaz[a], I. Yalcin[b], S. Okten[c], F. K. Onurdag[c] and E. Aki-Yalcin[b]

[a]Pharmaceutical Chemistry Department, Faculty of Pharmacy, Trakya University, Edirne, Turkey; [b]Pharmaceutical Chemistry Department, Faculty of Pharmacy, Ankara University, Ankara, Turkey; [c]Pharmaceutical Microbiology Department, Faculty of Pharmacy, Trakya University, Edirne, Turkey

ABSTRACT

Acinetobacter baumannii has emerged as an important pathogen for nosocomial infections having high morbidity and mortality. This pathogen is notorious for antimicrobial resistance to many common antimicrobial agents including fluoroquinolones, which have both intrinsic and acquired resistance mechanisms. Fluoroquinolones targeting the bacterial topoisomerase II (DNA gyrase and Topo IV) show potent broad-spectrum antibacterial activity by the stabilization of the covalent enzyme–DNA complex. However, their efficacy is now being threatened by an increasing prevalence of resistance. Fluoroquinolones cause stepwise mutations in DNA gyrase and Topo IV, having alterations of their binding sites. Furthermore, the water–Mg^{+2} bridge, which provides enzyme–fluoroquinolone interactions, has a significant role in resistance. In this study, 13 compounds were synthesized as 1,4-benzoxazine derivatives which act as bacterial topoisomerase II inhibitors and their antibacterial activities were determined against multi-drug resistant *Acinetobacter* strains which have ciprofloxacin (CIP) resistant and GyrA mutation. Afterwards we performed docking studies with Topo IV (pdb:2XKK) of these compounds to comprehend their binding properties in Discovery Studio 3.5. The results of this study show significant conclusions to elucidate the resistance mechanism and lead to the design of new antibacterial agents as bacterial topoisomerase II inhibitors.

ARTICLE HISTORY
Received 25 October 2017
Accepted 8 November 2017

KEYWORDS
Acinetobacter baumannii; benzoxazine; Ciprofloxacin; DNA gyrase; molecular docking; topoisomerase IV

Introduction

One of the major clinical and public health problems during the lifetime of most people is the serious infections caused by bacteria having resistance to commonly used antibiotics [1]. In recent years, antimicrobial resistance has steadily increased among Gram-positive and Gram-negative pathogens in the hospital and in the community. *Enterococcus faecium*, *Staphylococcus aureus*, *Klebsiella pneumoniae*, *Acinetobacter baumannii*, *Pseudomonas aeruginosa* and *Enterobacter* species, also called 'ESCAPE' pathogens in hospital-acquired

CONTACT E. Aki-Yalcin esinaki@ankara.edu.tr

[$]Presented at the 9th International Symposium on Computational Methods in Toxicology and Pharmacology Integrating Internet Resources, CMTPI-2017, 27–30 October 2017, Goa, India.

infections, have caused serious diseases and deaths [2]. In particular, nosocomial infections caused by multiple resistant strains of *Acinetobacter* spp. show resistance to many antimicrobial agents which include fluoroquinolones according to the intrinsic and acquired resistance mechanism. The failure of antibiotic therapy [3–5] is because of this multidrug resistance. In bacterial topoisomerase II enzymes of *Acinetobacter* spp., resistance to fluoroquinolones caused by spontaneous mutations of genes in the quinolone resistance-determining region (QRDR) generally cause resistance [3].

Topoisomerase enzymes which are essential for survival of the cells catalyse changes in DNA topology and they are found in all cell types. They are also well-known targets of antibacterial drugs. These proteins can be separated into two types, Topo I and Topo II, of which Topo I catalyses reactions by the transient break of one strand, whereas Topo II does this job by breaking two strands [6]. Heterotetrameric proteins such as DNA gyrase and its close relative Topo IV are from bacterial type topoisomerase II. DNA gyrase consists of two GyrA and two GyrB (A_2B_2) sub-units and Topo IV consists of two ParC (GrlA) and two ParE (GrlB) sub-units (C_2E_2) homologously to GyrA and GyrB, respectively. Whereas the GyrA and ParC sub-units are located in the DNA transit and they contain the active-site tyrosine, which is responsible for DNA cleavage, and they interact with DNA, the GyrB and ParE sub-units involve the ATPase active site [7,8]. Supercoiling DNA gyrase is responsible for the initiation and prolongation of transcription and for bacterial replication, by regulating the DNA. Topo IV decatenates chromosomal discrimination and resolution of DNA strands following DNA replication and can also relax supercoiled DNA [9]. DNA gyrase and Topo IV enzymes can relax both positive and negative DNA supercoils, but only the DNA gyrase enzyme can produce a negative supercoil by ATP (adenosine triphosphate) hydrolysis [7].

DNA gyrase and Topo IV are very similar to each other in structure, with similar molecular weights and very few sequence differences. In the heterotetramer structure (A_2B_2), the heart-shaped protein DNA with a large gap in its centre has a symmetrical axis between two GyrA and GyrB (ParC and ParE in Topo IV). GyrB and ParE sub-units are composed of three domains: GHKL (Gyrase, Hsp90, Histidine Kinase, MutL) domain, which is a part of many ATP-binding proteins; the second domain is responsible for transduction of ATP energy (transducer); and the TOPRIM (TOpoisomerase/PRIMase) domain, which connects between the enzyme and DNA [10,11]. On the other hand, GyrA and ParC sub-units consist of four domains: the winged helix domain (WHD), which contains the binding proteins of the nucleic acids (catalytic tyrosine); the tower domain; the long domain, classified as a coiled-coil; and the variable C-terminus [12]. Between the GyrA/B or ParC/E sub-units, in the form of A_2B_2 dimers, there are three gates which have a crucial role in the function of the enzymes. These are the N-gate or ATP gate formed by the GHKL domain of GyrB; the DNA gate consisting of TOPRIM and the C-gate formed between the coiled-coil domain of GyrA (Figure 1) [9].

DNA supercoiling by DNA gyrase begins with the G segment of the DNA interacting with the N-terminal end of the enzyme and moving towards the TOPRIM domain of GyrB, creating a positive supercoil of about 130 bases around the enzyme [13]. This spinning towards the C-terminal end facilitates the T-segment of the same DNA molecule reaching the N-gate and allows the G-segment to take its ready position for intercalating DNA strands [14]. The binding of ATP causes the N gate to be closed and caught of the T segment. The enzyme cuts DNA-phosphotyrosyl bonds by seperating four base pairs in G segment, creating double breaks in the DNA chain and covalent binding between GyrA and DNA. On this, the T-segment goes through the open DNA gate and the cleaved G-segment through the C-gate and is

accompanied by ATP binding and hydrolysis. The adenosine diphosphate (ADP), which is released by the hydrolysis of ATP, opens the N gate and makes the enzyme ready for a new supercoiling cycle (Figure 2) [7]. As a result, one gyrase supercoiling cycle introduces two negative supercoils into the DNA molecule at the expense of two ATPs [15]. If there is not enough ATP in the medium, DNA gyrase, especially by the reverse mechanism, can catalyse relaxation of negatively supercoiled DNA [16].

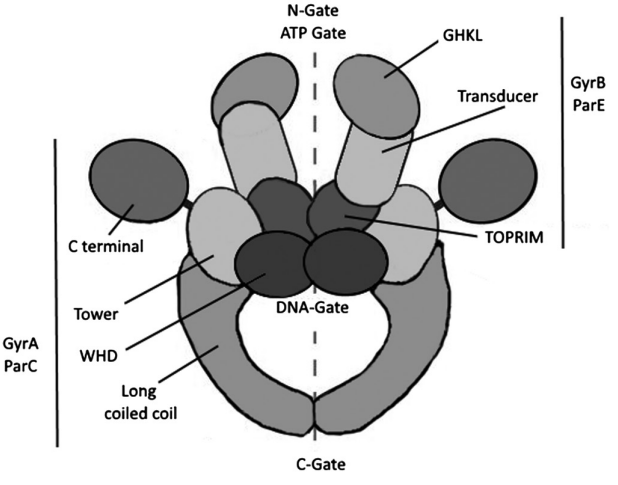

Figure 1. Structure of bacterial Topoisomerase II enzyme.

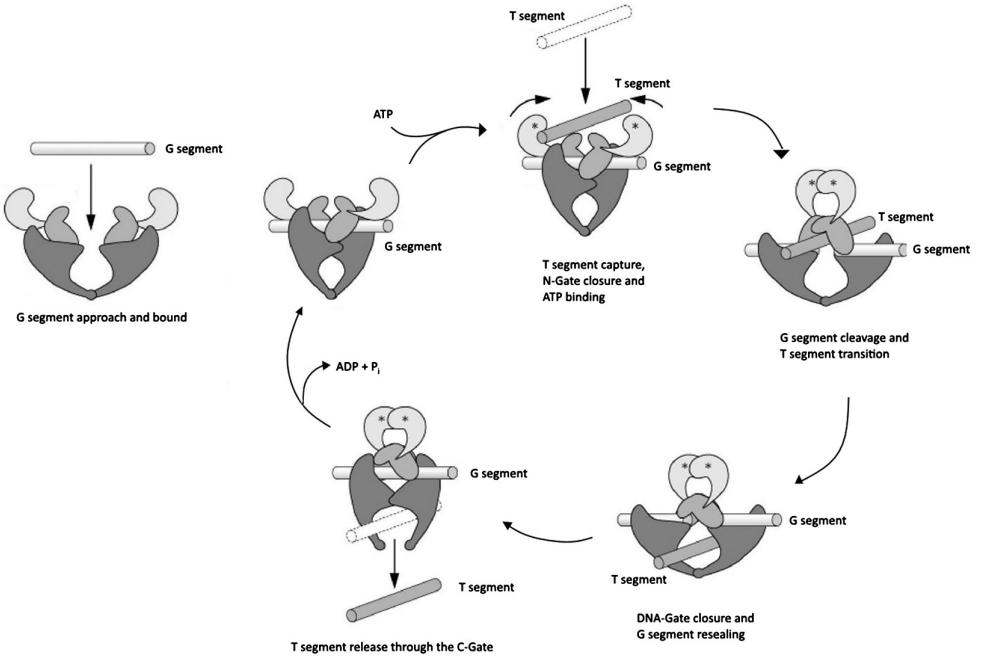

Figure 2. Mechanism of the interaction of DNA gyrase with DNA supercoiling (adapted from [16]).

Bacterial topoisomerase II enzymes require bivalent metal ions to display their catalytic activity. Mg^{+2} is a physiological divalent metal ion for bacterial topoisomerase II enzymes, but other divalent metal ions can also be used as a cofactor to catalyse the reactions performed by the enzymes [17]. The reactions of breaking the DNA chain by DNA gyrase and Topo IV enzymes are catalysed by the 'Dual Metal-Ion Mechanism'. According to this mechanism, the Mg^{+2} ion in the metal binding site A allows the DNA strands to pass through one to another, while in the metal binding site B region the Mg^{+2} ion fixes the –1 charged of phosphate. The intercalation reaction of DNA strands is completed by both of Mg^{+2} ions acting simultaneous [18,19].

Fluoroquinolones are DNA gyrase and Topo IV inhibitors that are frequently used in clinical therapy. They can also exhibit antibacterial activity by inhibiting DNA replication, as well as DNA damage, synthesis of uncompleted proteins, induction of oxidative damage and trigger off cell death mechanisms [20]. These compounds make covalent bonding with tyrosine in the active site of GyrA to stabilize cleaved DNA. Thus, fluoroquinolones that are bound to the enzyme-DNA complex separate the DNA strands from each other and constitute a physical barrier to the RNA polymerase and DNA helicase, thus triggering a series of events that result in cell death [21]. The interaction of fluoroquinolones with DNA and bacterial topoisomerase II enzymes has been elucidated by various crystallographic studies on DNA gyrase and Topo IV enzymes [13,22,23]. Investigations of the interaction of moxifloxacin complexing with DNA and Topo IV through *Acinetobacter baumannii* bacteria revealed that the quinolone ring of moxifloxacin interacted with the previous or subsequent bases of the DNA cleavage region via van der Waals and π–π interactions. In addition, it has been found that the Mg^{+2} ion located between the ParC region and moxifloxacin is also required for interaction. The water molecules surrounding the Mg^{+2} ion make hydrogen bonds with Ser84 and Glu88 in the part of the ParC that play a crucial role in the quinolone resistance [24].

The goal of this present study was to synthesize some novel 1,4-benzoxazine derivatives and to develop new and effective antibacterial agents against multi-drug resistant *Acinetobacter baumannii* strains and then to examine the structure activity relationships by using molecular modelling techniques with the description of the binding site features of 1,4-benzoxazine derivatives on *A. baumannii* showing ciprofloxacin (CIP) resistance and GyrA mutation.

Materials and methods

Tested compounds

To investigate their inhibitory antibacterial activity against multidrug resistant *A. baumannii*, we tested novel synthesized 1,4-benzoxazine (5a–m) derivatives, which are holding different substituents in R positions in their structure, as given in Figure 3.

Chemistry

All chemicals and solvents were purchased from commercial vendors and were used without further purification. The progress of the reaction was monitored on ready-made silica gel plates (Merck, Germany). The melting points were measured with a capillary melting point apparatus (Buchi, Switzerland B540) and were uncorrected. Yields were calculated after

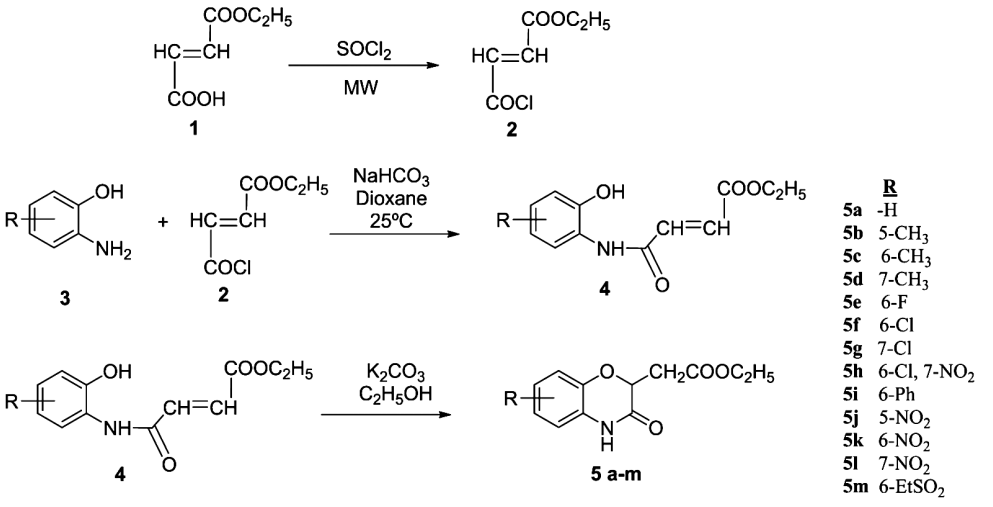

Figure 3. Synthesis of 1,4-benzoxazine derivatives.

recrystallization. The ^{1}H-NMR spectra were recorded employing a VARIAN Mercury 400-MHz FT spectrometer, chemical shifts (*d*) were in parts per million relative to tetramethylsilane (TMS) and coupling constants (*J*) were reported in hertz. Mass spectra were taken on a Waters Micromass ZQ using the electrospray ionization (ESI) method. Elemental analyses were performed by Leco CHNS-932 CHNS-O analyser. The result of the elemental analyses (C, H, N, S) were within ±0.4% of the calculated amounts.

General procedure for the preparation of ethyl 2-(3-oxo-3,4-dihydro-2H-1,4-benzoxazin-2-yl)acetate derivatives

Monoethyl fumaric acid (1) (10 mmol) and thionyl chloride (5 mmol) reacted under 150 watt microwave conditions for 10 min at 100°C in benzene (5 ml). At the end of the reaction, excess thionyl chloride was evaporated. Obtained monoethyl fumaryl chloride (2) was added dropwise to a suspension of appropriate substituted-2-aminophenols (3) (10 mmol) and $NaHCO_3$ (10 mmol) in dioxane. The substituent types and positions of 2-aminophenols varies according to the final products obtained. As an example; for the preparation of 7-methyl substituted 'ethyl 2-(3-oxo-3,4-dihydro-2H-1,4-benzoxazin-2-yl)acetate' (5d), 5-methyl substituted '2-aminophenol', has been chosen etc. Then the reaction mixture was stirred for 24 h at room temperature, then poured into water and extracted with ethyl acetate (15 ml). The extract was washed with water, dried and evaporated, respectively. The residue was recrystallized from EtOH to give 4 ethyl 3- [(4- and/or 5-substituted-2-hydroxyphenyl)carbamoyl]acrylate (4) derivatives. A suspension of these compounds (10 mmol) and K_2CO_3 (5 mmol) in EtOH (70 ml) was stirred for 3 h at room temperature. The reaction mixture was poured into water and extracted with ethyl acetate (15 ml). The extracts were washed with water, dried and evaporated, respectively (Figure 3) [25]. The residues were recrystallized from EtOH and obtained ethyl 2-(3-oxo-3,4-dihydro-2H-1,4-benzoxazin-2-yl)acetate (5a–m) derivatives.

Microbiology

Antibacterial activities of synthesized compounds were determined as MIC values using microdilution method 1, against *Klebsiella pneumoniae* ATCC 700603, *Klebsiella pneumoniae* RSKK 576, *Pseudomonas aeruginosa* ATCC 10145, *Escherichia coli* ATCC 25922, *Staphylococcus aureus* ATCC 29213, *Enterococcus faecalis* ATCC 29212 and clinical isolates of *Acinetobacter baumannii* obtained from the Trakya University Medical Faculty Hospital Microbiology Laboratory.

A. baumannii gyrA, parC and gyrB genes were amplified using gyrA_F 5′-AAATCTGCCCGTGTCGTTGGT-3′, gyrA_R 5′-GCCATACCTACGGCGATACC-3′, gyrB_F 5′-GTGCGCGCTTTGATAAAAT-3′, gyrB_R 5′-ACAGTTACACGTGGCCAGTA-3′, parC_F 5′ATGAGCGAGCTAGGCTTAAA-3' and parC_R 5′-TTAAGTTGTCCTTGCCATTCA-3' primers by applying qPCR techniques to ciprofloxacin-resistant *Acinetobater baumannii* clinical isolates encoded as A3, A5, C5, B4, B1, C6, D1, D2, D3 and D6. High-resolution melting (HRM) analyses were performed to group the gyrA, gyrB and parC gene quantitative polymerase chain reaction (qPCR) amplicons according to their DNA sequences. HRM analysis was performed in order to group the gene sequences amplified from different isolates by qPCR according to their DNA sequences.

Newly synthesized compounds' antibacterial activity with the presence of ciprofloxacin were tested again using microdilution method 2, against clinical Acinetobacter isolates which are obtained from Trakya University Medical Faculty Hospital Microbiology Laboratory, resistant to ciprofloxacin and mutated in the gyrA gene region determined by q-PCR techniques.

Susceptibility testing was performed according to the guidelines of the Clinical and Laboratory Standards Institute (CLSI) M100-S25 and M27-A3.

Microdilution method 1

Stock solutions of the test compounds were dissolved in dimethylsulphoxide (DMSO). Standard antibiotic solutions were dissolved in the appropriate solutions according to the CLSI M100-S25 recommendations. The colonies produced in culture plates were transferred to Mueller Hinton Broth (MHB) from Mueller Hinton Agar (MHA) for bacteria and to Sabouraud Dextrose Agar (SDA) from Sabouraud Liquid Medium (SLM) for yeasts, respectively. The bacterial suspensions used for inoculation were prepared at 10^5 CFU/mL by diluting fresh cultures at McFarland 0.5 density. Suspensions of the yeast at McFarland density was diluted 1:100 and 1:20, respectively, and 2.5×10^3 CFU/mL were inoculated to the 2-fold-diluted solution of the compounds. Standard drugs and stock solutions of the tested compounds were diluted 2-fold in the wells of the microplates such as the solution of the standard drugs were prepared at 16, 8, 4, 2, 1, 0.5, 0.25, 0.125, 0.0625, 0.03125, 0.015625 and 0.0078 µg/mL concentrations and the synthesized compounds were prepared at 512, 256, 128, 64, 32, 16, 8 and 4 µg/mL concentrations. A 10 µl micro-organism inoculum was added to each well of the microplates. Microplates including bacteria were incubated at 37°C for 16–20 h. The lowest concentration of the compounds that completely inhibits macroscopic growth was determined after incubation and reported as the minimum inhibitory concentration (MIC).

Microdilution method 2

Stock solutions of the test compounds and ciprofloxacin were dissolved in DMSO and water, respectively. Cation-adjusted MHB was used in the study. Passages were made from *A.*

baumannii colonies grown on MHA plaques to MHB media and liquid media were incubated for 16–20 h at 37°C. Culture was adjusted to McFarland 0.5 density by adding liquid medium to the culture to reach the inoculum. The bacterial suspensions used for inoculation were prepared at 10^5 CFU/mL by diluting fresh cultures at McFarland 0.5 density. Ciprofloxacin dilutions were prepared for use with each compound using the stock solution of ciprofloxacin. Then, 100 µL of the medium containing the fixed amount of the prepared compound was added to wells containing ciprofloxacin and 100 µL of the medium. Ciprofloxacin susceptibility was investigated in accordance with the CLSI M100-S25 (2015) standards using the medium containing the substance at half the concentration of the previously determined MIC values of the compounds. The results were considered significant when 4-fold excess reduction was detected between the MIC value of ciprofloxacin and the MIC value of the combination of compound-ciprofloxacin. Stock solutions of the tested compounds and standard drugs were diluted 2-fold in the wells of the microplates, so the solutions of the synthesized compounds were half MIC concentrations and ciprofloxacin were prepared at 16, 8, 4, 2, 1, 0.5, 0.25, 0.125, 0.0625, 0.03125, 0.015625 and 0.0078 µg/mL concentrations. A 10 µl micro-organism inoculum was added to each well of the microplates. Microplates including bacteria were incubated at 37°C for 16–20 h. All solvents and diluents, pure micro-organisms and pure media were used in control wells. After incubation, the lowest concentration of the compounds that completely inhibits macroscopic growth was determined and reported as the MIC.

Computational methods

Preparation of ligands

The 3D structures of a set of synthesized 1,4-benzoxazine derivatives (5a–m), which are given in Figure 3, as well as the antibiotic moxifloxacin, were sketched using the Accelrys Discovery Studio (DS) 3.5 [26] Sketch Molecules module. The geometries of these compounds were subsequently optimized using the Minimization module of DS 3.5 using the CHARMm force field and Adopted basis Newton-Raphson method with the root mean deviation (RMS) gradient was < 0.05 kcal/mol/Å^2.

Preparation of protein

The crystal structure of the Topo IV with crystal structure of moxifloxacin in *A. baumannii* was retrieved from the Protein Data Bank (pdb: 2XKK) [24]. DS 3.5 software was used for preparation of protein. Protein reports were extracted and the missing parts of the proteins were identified and these parts were completed through fragments. Using the software's automatic protein preparation unit, proteins were prepared and invalid residues were detected and corrected. The prepared protein was taken, the ligand was extracted, hydrogens were added and their positions were optimized using the all-atom CHARMm forcefield parameterization, which was assigned and then minimized using the adopted basis Newton-Raphson (ABNR) method as described above. The minimized protein was defined as the receptor using the binding site module. The binding site was defined to encompass around the ligand (moxifloxacin) inside the protein which accommodated all the important interaction residues in the active site of the enzyme. The binding sphere for 2XKK (–19.15, 45.83, –14.48, 14.99) was selected from the active site using the binding site tools (Figure 4(a)).

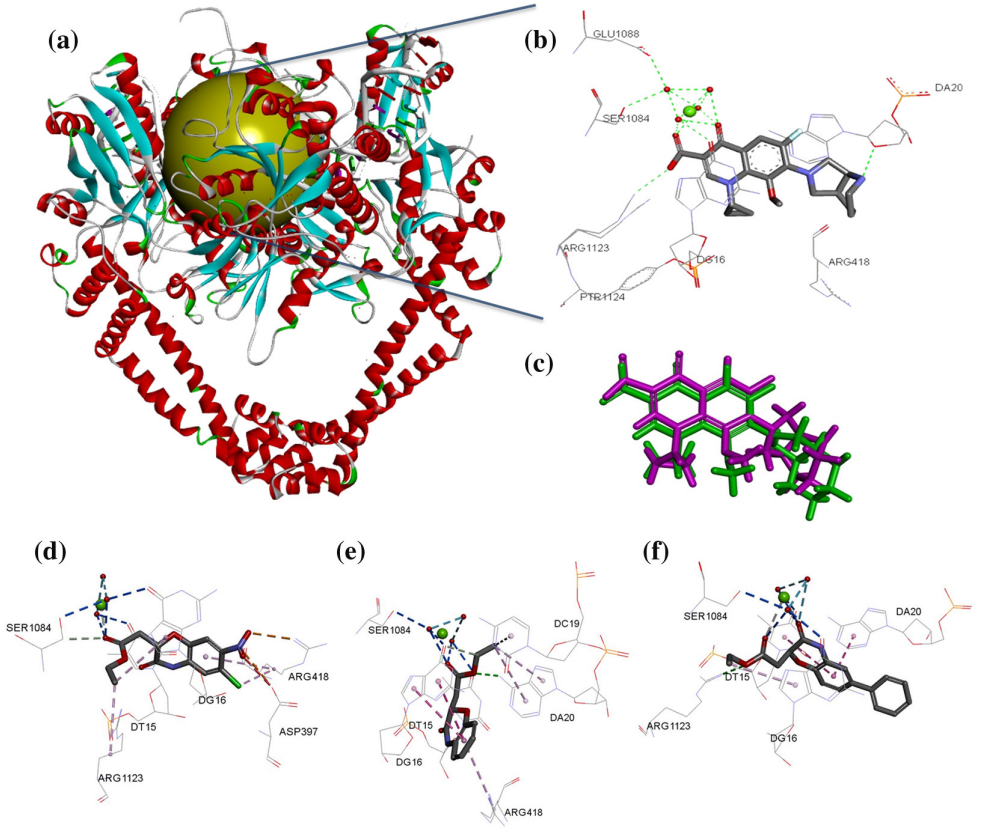

Figure 4. The performed docking poses. (a) The structure of Topo IV ParC sub-unit showing the selected binding sphere used in our docking studies. The binding sphere coordinates; −19.15, 45.83, −14.48, radius; 14.9915. (b) Water–metal ion bridge that mediates critical interactions between moxifloxacin and Topo IV. Moxifloxacin interacts with Ser84 via water molecules around the Mg^{+2} ion. (c) Structural superimposition of the docked moxifloxacin (green) and from the X-ray structure (pink) with 0.9631 RMSD value. (d) Docked position of compound 5a. (e) Docked position of compound 5h. (f) Docked position of compound 5i.

Molecular docking

CDOCKER [25], that is a CHARMm-based grid-enabled docking method, was performed by using DS 3.5 software. The CDOCKER method uses soft core potentials and molecular dynamics generated random ligand conformations and poses refinement in the active site using a simulated annealing process. The protein is held rigid, while the ligands are allowed to be flexible during refinement [27]. The docking process and scoring methodology were first validated by docking of moxifloxacin. The docked position of moxifloxacin overlaps well with the crystal structure position, with an RMSD of 0.9631 Å (Figure 4(c)). Afterwards, molecular docking studies were performed on the tested compounds 5a–m.

The docking parameters were as follows: Top Hits: 10; Random Conformations: 10; Random Conformations Dynamics Step: 5000; Dynamics Target: 1000; Grid Extension: 8.0; Random Dynamics Time Step: 0.002.

Results and discussion

Chemistry

In this study, a total of 13 ethyl 2-(3-oxo-3,4-dihydro-2H-1,4-benzoxazin-2-yl)acetate (5a–m) derivatives were synthesized and five of them (5b, 5g, 5i, 5j, 5m) were original. The other eight compounds (5a, 5c–f, 5h, 5k, 5l) were synthesized before by our group and some other research groups for the first time and related articles [25,28–30] are indicated at Table 1. We synthesized five novel compounds carrying various kinds of groups/atoms having different physicochemical properties attached to the benzene ring of benzoxazine to observe the effects on the biological activity. For synthesis of ethyl 2-(3-oxo-3,4-dihydro-2H-1,4-benzoxazin-2-yl)acetate derivatives, mono ethyl fumaric acid and thionyl chloride reacted under microwave conditions. Obtained monoethyl fumaryl chloride was mixed with substituted-2-aminophenols and $NaHCO_3$ in dioxane. A suspension of obtained compounds and K_2CO_3 in EtOH was stirred for 3 h at room temperature to achieve ethyl 2-(3-oxo-3,4-dihydro-2H-1,4-benzoxazin-2-yl)acetate derivatives (5a–m), as given in Figure 3 [23]. The purity of the synthesized compounds has been controlled by thin layer chromatography (TLC) and their melting points were determined. Their structures were elucidated by using ^{1}H-NMR, Mass and Elemental Analysis methods and results are in agreement with the proposed structures, as given in Table 1.

According to the spectroscopic data of the compounds 5a–m; the ^{1}H-NMR spectra of the compounds; the CH_3 protons and the -CH_2 protons of the ethyl ester in the second position of the benzoxazine ring were observed as triplets at 1.05–1.30 ppm and as quartets at 4.1–4.4 ppm, respectively. The -CH_2- bridge between the benzoxazine ring and the ester structure was observed in the range of 2.9–3.3 ppm, giving the doublet separately. Besides, the -H in the second position of the benzoxazine ring was observed as a doublet of doublets at 4.9–5.1 ppm. Moreover, all the aromatic protons were observed at 6.7–8.1 ppm and the –NH proton in amide structure appeared at 8–11 ppm as a singlet. Mass spectra of the compounds showed M^++H or M^+–H peaks in accordance with their formulas, since the electrospray ionization (+) and (–) methods were employed. On the other hand, the results of the elemental analyses (C, H, N, S) were within ±0.4% of the calculated amounts.

Microbiology

The *in vitro* antibacterial activity of the synthesized compounds (5a–m) was observed against some Gram-negative bacteria such as *Klebsiella pneumoniae* ATCC 700603, *Pseudomonas aeruginosa* ATCC 10145, *Escherichia coli* ATCC 25922, some Gram-positive bacteria such as *Staphylococcus aureus* ATCC 29213, *Enterococcus faecalis* ATCC 29212 and their clinical isolates. The synthesized compounds (5a–m) displayed poor intrinsic antibacterial activity at the MIC values between 64–512 µg/ml, as given in Table 2.

For the antibacterial activity test against *Acinetobacter baumannii* clinical isolates, which are ciprofloxacin (CIP) resistant and Ser84 (TCA) to Leu84 (TTA) mutation in GyrA, 1,4-benzoxazine derivatives (5a–m) were first tested alone and it was observed that they did not exhibit any significant intrinsic antibacterial activity, showing MIC values between 128 and 512 µg/ml. Afterwards they were tested at half of their concentrations of the observed MIC

Table 1. Physical and spectral data of the synthesized 1,4-benzoxazine derivatives (5a–m).

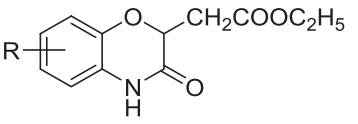

5 a-m

							Calculated element (%)	
	R	*m.p. (°C)*	*Yield (%)*	*^{1}H-NMR (δ ppm, J=Hz)*	*MASS m/e (%X)*	*Molecular formula*	*found element (%)*	*Reference*
5a	-H	112–113	63.7	1.17 (t, 3H); 2.84–3.00 (dd, H, *J* =6.8; 7.2; dd, H, *J* =4.8; 4.4); 4.08 (q, 2H); 4.9 (dd, 1H, *J* =4.8; 4); 6.87–6.96 (m, 4H); 10.74 (s, 1H)	236.1 (M^++H) (%50)	$C_{12}H_{13}NO_4$	C: 61.27 H: 5.57 N: 5.95 C: 61.09 H: 5.44 N: 6.13	
5b	5-CH_3	131–134	63.6	1.28 (t, 3H); 2.24 (s, 3H); 2.91–3.14 (dd, H, *J* =7.6; 8; dd, H, *J* =4.8; 4.4); 4.21 (q, 2H); 4.9 (dd, 1H, *J* =4.4); 6.87–6.69 (m, 3H); 7.77 (s, 1H)	250.3 (M^++H) (%10)	$C_{13}H_{15}NO_4$	C: 62.64 H: 6.07 N: 5.62 C: 62.68 H: 6.28 N: 5.84	
5c	6-CH_3	115–117	76.3	1.28 (t, 3H); 2.28 (s, 3H); 2.91–3.13 (dd, H, *J* =7.6; dd, H, *J* =4; 4.4); 4.21 (q, 2H); 4.95 (dd, 1H, *J* =4.4); 6.60 (s, 1H,); 6.77 (d, 1H, J_o = 8; J_m = 1.2); 6.85 (d, 1H, J_o = 8); 8.049 (s, 1H)	250.3 (M^++H) (%10)	$C_{13}H_{15}NO_4$	C: 62.64 H: 6.07 N: 5.62 C: 62.51 H: 6.05 N: 5.85	[28]
5d	7-CH_3	124–125	62.6	1.27 (t, 3H); 2.27 (s, 3H); 2.90–3.12 (dd, H, *J* =7.6; dd, H, *J* =4; 3.6); 4.21(q, 2H, 6); 4.96 (dd, 1H, *J* =4.4; 4); 6.67 (d, 1H, J_o = 8); 6.76 (d, 1H, J_o = 8); 6.78 (s, 1H); 8.20 (s, 1H)	248.4 (M^+-H) (%100)	$C_{13}H_{15}NO_4$. $0.1H_2O$	C: 62.64 H: 6.07 N: 5.62 C: 62.51 H: 6.11 N: 5.81	[28]
5e	6-F	120–121	80.4	1.17 (t, 3H); 2.85–3.00 (dd, H, *J* =7.2; 6.8; dd, H, *J* =4.4); 3.32 (s, 1H); 4.08 (q, 2H); 4.90 (dd, 1H, *J* =4; 4.4); 6.67–6.71 (m, 1H); 6.74 (dd, 1H, J_{oF} = 8.8; 9.2; J_m = 2.8; 3.2); 6.92 (dd, 1H, J_o = 8.8; 9.2; J_{mF} = 4.8; 5.2)	252.3 (M^+-H) (%100)	$C_{12}H_{12}FNO_4$. $0.1H_2O$	C: 56.92 H: 4.78 N: 5.53 C: 56.47 H: 4.74 N: 5.76	[29]
5f	6-Cl	150–151	75.7	1.29 (t, 3H); 2.96–3.14 (dd, H, *J* =6.8; 7.2; dd, H, *J* =4.4); 4.22 (q, 2H); 4.97 (dd, 1H, *J* =4.4); 6.84 (d, 1H, J_m=2.4); 6.88 (d, 1H, J_o = 8.8); 6.93 (dd, 1H, J_o = 8.8; J_m = 2; 2.4); 8.20 (s, 1H)	270.3 (M^++H) (%50)	$C_{12}H_{12}ClNO_4$	C: 53.44 H: 4.49 N: 5.19 C: 53.24 H: 4.23 N: 5.50	[25,28,30]

5g	7-Cl	161–163	56.9	1.17 (t, 3H); 2.88–3.00 (dd, H, J =6; 6.4; dd, H, J =4.8; 4.4); 4.08 (q, 2H); 4.97 (dd, 1H, J =4.8; 4.4); 6.88 (d, 1H, J_o = 8.8); 6.99–7.02 (m, 2H); 10.85 (s, 1H)	268.3 (M^+-H) (%100)	$C_{12}H_{12}ClNO_4$	C: 53.44 H: 4.49 N: 5.19 C: 53.18 H: 4.30 N: 5.26	
5h	6-Cl,7-NO_2	172–173	73.1	1.28 (t, 3H); 3.10–3.12 (m, 2H); 4.21 (q, 2H); 5.05 (t, 1H); 6.96 (s, 1H); 7.64 (s, 1H); 8.81 (s, 1H)	315.2 (M^+-H) (%100)	$C_{12}H_{11}ClN_2O_6$	C: 45.80 H: 3.52 N: 8.90 C: 45.66 H: 3.33 N: 8.95	[25,28]
5i	6-Ph	152–153	87.5	1.16 (t, 3H); 2.87–3.01 (dd, H, J =6.8; dd, H, J =4.8; 4.4); 4.08 (q, 2H); 4.94 (t, 1H); 6.97 (d, 1H, J_o = 8.4); 7.13 (d, 1H, J_m = 2.4); 7.18 (dd, 1H, J_o = 8; J_m = 2.4); 7.31 (t, 1H); 7.43 (t, 2H); 7.52 (d, 2H, J_o = 8); 10.81 (s, 1H)	310.2 (M^++H) (%100)	$C_{18}H_{17}NO_4$	C: 69.44 H: 5.50 N: 4.50 C: 69,45 H: 5,42 N: 4,78	
5j	5-NO_2	130–131	73	1.16 (t, 3H); 2.94–3.07 (dd, H, J =6.4; 6; dd, H, J =4.8); 4.08 (q, 2H); 5.09 (t, 1H); 7.131 (t, 1H); 7.36 (dd, 1H, J_o = 8.4; J_m = 0.8; 1.2); 7.76 (dd, 1H, J_o = 8; J_m = 1.2); 10.38(s, 1H)	279.3 (M^+-H) (%100)	$C_{12}H_{12}N_2O_6$	C: 51.43 H: 4.32 N: 10.00 C: 51.05 H: 4.21 N: 9.82	
5k	6-NO_2	185–187	74.7	1.27(t, 3H); 3.07–3.18 (dd, H, J =6; dd, H, J =4.8); 4.20 (q, 2H); 5.10 (t, 1H); 7.03 (d, 1H, J_o = 8.8); 7.73 (d, 1H, J_m = 2.8); 7.90 (dd, 1H, J_o = 9.2; J_m = 2.4; 2); 8.68 (s, 1H)	279.2 (M^+-H) (%100)	$C_{12}H_{12}N_2O_6$	C: 51.43 H: 4.32 N: 10.00 C: 51,34 H: 4,45 N: 9,90	[30]
5l	7-NO_2	177–178	73.6	1.28 (t, 3H); 3.17–3.04 (dd, 1H, J =6; dd, 1H, J =4); 4.21 (q, 2H); 5.06 (dd, 1H, J =4.4); 6.90 (d, 1H, J_o = 8.8); 7.86 (d, 1H, J_m = 2.4); 7.91 (dd, 1H, J_o = 8.4; J_m = 2; 2.8); 8.69 (s, 1H)	281.4 (M^++H) (%50)	$C_{12}H_{12}N_2O_6$	C: 51.43 H: 4.32 N: 10.00 C: 51.24 H: 4.37 N: 9.62	[25,28]
5m	6-$EtSO_2$	110–114	59	1.25–1.30 (m, 6H); 3.16–3.04 (m, 4H); 4.21(q, 2H); 5.07 (dd, 1H, J =4.4); 7.52–7.08 (m, 3H); 7.09 (d, 1H, J_o = 8.8); 7.38 (d, 1H, J_m = 2); 7.51 (dd, 1H, J_o = 8.4; J_m = 2); 8.65 (s, 1H)	326.1 (M^+-H) (%100)	$C_{14}H_{17}NO_6S$	C: 51.37 H: 5.23 N: 4.28 S: 9.80 C: 51.09 H: 5.62 N: 4.44 S: 9.62	

values in combination with CIP against the same bacterial strains, a reversal in the antibacterial activity of CIP with up to 16/18-fold better MIC values was observed, as shown in Table 3.

As a result of the measured synergism test of the 1,4-benzoxazine derivatives, it was found that the compounds 5h, 5a and 5i provided the most significant contribution in the reversal of antibacterial activity of CIP among the tested compounds, with the MIC values of 0.0156, 0.0312 and 0.0312 µg/ml, respectively.

Molecular docking

It was found that the synthesized 1,4-benzoxazine derivatives (5a–m) were interacting with the enzyme with binding energies between –6805.34 and –6823.36 kcal/mol as a result of docking of the Topo IV enzyme, ParC sub-unit (pdb:2XKK) as given in Table 4.

The coordination of the hydrogen bonds between the Mg^{+2} and Ser84 amino acids of the compounds is very important for antibacterial activity [24]. In addition, synthesized 1,4-benzoxazine derivatives (5a–m) form hydrogen bonds with important amino acids Ser84, Arg123 and Ptr124 and increase their interactions with the enzyme.

All of the 1,4-benzoxazin derivatives (5a–m) were found to interact with the Mg^{+2} ion and Ser84 amino acid via water molecules. It has been determined that 5c, 5i and 5m of the compounds make a direct hydrogen bond with Arg123 amino acid and 5m with Ptr124 amino acid.

The most active compound, 5h, forms hydrogen bonds with important amino acid Ser84 via water molecules, π interactions with DG16, amino acid Arg418 and 2.35 Å distance to Mg^{+2} ion (Figure 4(e)). Compound 5a forms direct hydrogen bonds with DA20 and Ser84 via water molecules, π interactions with DG16, DC19 and DA20, amino acid Arg418 and 2.34 Å

Table 2. *In vitro* antimicrobial activities of ethyl 2-(3-oxo-3,4-dihydro-2H-1,4-benzoxazin-2-yl)acetate (5a–m).

		Micro-organisms									
		Gram-negative bacteria						*Gram-positive bacteria*			
Compounds	*R*	*K.p*	*K.p**	*E.c*	*E.c**	*P.a*	*P.a**	*S.a*	*S.a**	*E.f*	*E.f**
5a	-H	256	256	256	128	128	128	256	256	256	64
5b	5-CH_3	256	256	256	128	256	128	256	256	256	256
5c	6-CH_3	256	256	256	256	256	128	256	256	256	256
5d	7-CH_3	256	256	256	256	256	128	256	512	256	256
5e	6-F	256	256	256	256	256	128	256	512	256	128
5f	6-Cl	256	256	256	128	256	128	256	512	256	128
5g	7-Cl	256	256	256	256	256	128	256	256	256	128
5h	6-Cl, 7-NO_2	128	128	128	128	128	64	256	256	128	128
5i	6-Ph	128	64	128	128	128	64	128	128	64	128
5j	5-NO_2	128	64	128	128	128	64	256	512	128	128
5k	6-NO_2	128	128	128	128	128	64	256	128	128	128
5l	7-NO_2	128	128	128	128	128	64	256	256	128	128
5m	6-$EtSO_2$	128	64	128	128	128	64	256	256	128	128
Ampicillin		—	—	4	16	—	—	1	16	0.5	> 16
Cefuroxime		> 16	0.25	4	> 16	—	—	0.5	> 16	—	—
Ciprofloxacin		0.5	< 0.125	0.0156	> 16	1	8	0.125	> 16	0.5	> 16
Imipenem		0.5	0.0078	0.25	0.0625	0.5	< 0.0078	0.0156	> 16	0.5	> 16
Meropenem		0.5	0.0156	0.0625	0.0078	0.5	< 0.0078	0.0156	> 16	2	—

K.p, *K. pneumoniae* ATCC 700603; K.p*, *K. pneumoniae* RSKK 576; E.c, *E. coli* ATCC 25922; E.c*, *E. coli izolat* (ESBL); P.a, *Pseudomonas aeruginosa* ATCC 10145; P.a*, *P. aeruginosa* isolate; S.a, *Staphylococcus aureus* ATCC 29213; S.a*, *S. aureus* isolate (MRSA); E.f, *Enterococcus faecalis* ATCC 29212; E.f*, *E. faecalis* isolate (VRE).

Table 3. Combination of compounds and CIP observed MIC values (μg/ml) tested against *A. baumannii* clinic isolates.

	Acinetobacter baumannii clinic isolates									
MIC values	*A3*	*A5*	*C5*	*B4*	*B1*	*C6*	*D1*	*D2*	*D3*	*D6*
	CIP	*CIP*	*CIP*	*CIP*	*CIP*	*CIP*	*CIP*	*CIP*	*CIP*	*CIP*
	MIC: 8	*MIC: 8*	*MIC: 16*	*MIC: 8*	*MIC: > 16*	*MIC: 8*	*MIC: 8*	*MIC: 8*	*MIC: 8*	*MIC: 8*
	CIP+	*CIP+*	*CIP+*	*CIP+*	*CIP+*	*CIP+*	*CIP+*	*CIP+*	*CIP+*	*CIP+*
(μg /mL)	*compound*	*compound*	*compound*	*compound*	*compound*	*compound*	*compound*	*compound*	*compound*	*compound*
16										
8										
4										
2										
1										
0.5										
0.25	5d, 5i			5a					5m	5b
0.125	5a, 5b, 5c, 5e, 5f, 5g, 5h, 5j, 5k, 5l, 5m	5a, 5b, 5c, 5d, 5e, 5f, 5g, 5h, 5i, 5j, 5k, 5l, 5m	5d	5b, 5c, 5d, 5e, 5f, 5g, 5h, 5i, 5j, 5k, 5l, 5m	1d	5b, 5c, 5e, 5f, 5g, 5j, 5l, 5m	5c, 5e, 5m,	5a, 5b, 5c, 5d, 5e, 5f, 5g, 5h, 5i, 5j, 5k, 5l, 5m	5a, 5b, 5c, 5d, 5e, 5f, 5g, 5h, 5i, 5j, 5k, 5l,	5a, 5c, 5d, 5e, 5f, 5g, 5h, 5i, 5j, 5k, 5l, 5m
0.0625			5a, 5b, 5c, 5e, 5f, 5g, 5h, 5i, 5j, 5k, 5l, 5m		5a, 5b, 5c, 5e, 5f, 5g, 5h, 5i, 5j, 5k, 5l, 5m	5d, 5k	5a, 5b, 5d, 5f, 5g, 5h, 5i, 5j, 5k, 5l			
0.0312						5a, 5i				
0.0156						5h				

Table 4. Molecular docking results of 1,4-benzoxazine derivatives (5a–m).

	R	*Binding energy*	*-CDocker Energy*	*H-bonds*	*H-bonds with HOH*	*Pi interactions*	*Mg distance (Å)*
5a	-H	−6,746.66	38.4688	DA20	Ser84, DG16, DT15	DG16[a], DC19[e], DA20[e], Arg418[e]	2.34
5b	5-CH_3	−6,741.1	34.7307	—	Ser84, DG16, DT15	DT15[e], DC19[a], DA20[a]	2.34
5c	6-CH_3	−6,745.46	42.1595	Arg123	Ser84, DG16, DT15	DT15[e], DC19[a,e], DA20[a,e]	2.27
5d	7-CH_3	−6,745.28	41.7145	—	Ser84, DG16, DT15	DG16[a], DC19[a], DA20[a]	2.26
5e	6-F	−6,734.67	35.024	Arg418	Ser84, DG16, DT15	DT15[a], DG16[a], DC19[a], DA20[e]	2.35
5f	6-Cl	−6,743.76	37.6106	—	Ser84, DG16, DT15	DT15[e], DG16[a]	2.37
5g	7-Cl	−6,743.84	35.2863	—	Ser84, DG16, DT15	DG16[g], DA20[e]	2.39
5h	6-Cl, 7-NO_2	−6,746.23	29.3661	—	Ser84, DG16, DT15	DG16[e], Arg418[e]	2.35
5i	6-Ph	−6,747.13	40.3719	Arg123	Ser84, DG16, DT15	DT15[a], DG16[e], DA20[a]	2.28
5j	5-NO_2	−6,755.5	31.8477	Gly419, Asp397	Ser84, DG16, DT15	DG16[e]	2.24
5k	6-NO_2	−6,750.56	31.5614	Arg418	Ser84, DG16, DT15	DG16[e], DC19[i], DA20[e], Arg418[h]	2.33
5l	7-NO_2	−6,744.74	38.7168	—	Ser84, DG16, DT15	DG16[a], DC19[a], DA20[a]	2.27
5m	6-$EtSO_2$	−6,737.05	40.2193	Arg418, Gly419, Ptr124, Arg123	Ser84, DG16, DT15	DT15[a], DG16[a], DA20[e]	2.53

Pi interactions; a: π–π, b: π–S, c: π–cation, d: π–anion, e: π–Alkyl, f: π–H bond donor, g: π–n, h:π–amide, i: π–σ.

distance to Mg^{+2} ion (Figure 4(d)). Compound 5i forms direct hydrogen bonds with amino acid Arg123 and Ser84 via water molecules, π interactions with DT15, DG16 and DA20 and 2.28 Å distance to Mg^{+2} ion (Figure 4(f)).

Conclusion

Bacterial topoisomerase II enzymes are divided into two groups; DNA gyrase and Topo IV. DNA gyrase provides the regulation of DNA supercoil, the initiation and prolongation of transcription and bacterial replication and Topo IV enzyme is responsible for DNA strand disassembly and chromosomal discrimination following by DNA replication. The inhibition of these enzymes, which have a very large prevalence in the life cycle of bacteria, is leading to bacterial cell death and the compounds that provide this effect also have a strong bactericidal effect. DNA gyrase/Topo IV enzymes require bivalent metal ions (Mg^{+2}) to be able to show their catalytic activity. DNA chain-breaking reactions are catalysed by the 'dual metal-ion mechanism' and, for this mechanism, two Mg^{+2} ion acting as cofactors should be able to simulate, simultaneously [17–19]. GyrA/ParC inhibitors interact with the Mg^{+2} ion and

Ser84 amino acid through water molecules during DNA replication. Coordination by hydrogen bonds between the inhibitor, Mg^{+2} and Ser84 amino acids prevents two Mg^{+2} ions from acting simultaneously [24], thus preventing DNA strands from passing through each other. Mutations on the Ser84 amino acid give rise to bacterial resistance, preventing this coordination from occurring.

In this study synthesized 1,4-benzoxazine derivatives (5a–m) did not exhibit any significant intrinsic antibacterial activity but, when they tested with a combination of CIP, a reversal in the antibacterial activity of CIP with up to 16/18-fold better MIC values was observed. This indicates that, when CIP is used in combination with the indicated concentrations of the compounds, the resistance is removed.

Molecular docking results showed that all of the synthesized 1,4-benzoxazine derivatives (5a–m) interacted with the Mg^{+2} ion and Ser84 amino acid through water molecules in the Topo IV enzyme. The antibacterial tests results as MIC values of CIP decreased at least 10-fold when used with a combination of synthesized compounds (5a–m). According to the results of this study, the resistance mechanism is explicated and the structural properties of the Topo IV inhibitors have been described to design new antibacterial agents.

Disclosure statement

The authors report no conflicts of interest. The authors alone are responsible for the content and writing of the paper.

References

[1] D.E. Ehmann and S.D. Lahiri, *Novel compounds targeting bacterial DNA topoisomerase/DNA gyrase*, Curr. Opin. Pharmacol. 18 (2014), pp. 76–83.

[2] H.W. Boucher, G.H. Talbot, J.S. Bradley, J.E. Edwards, D. Gilbert, L.B. Rice, M. Scheld, B. Spellberg, and J. Bartlett, *Bad bugs, no drugs: No ESKAPE! An update from the Infectious Diseases Society of America*, Clin. Infect. Dis. 48 (2009), pp. 1–12.

[3] S. Park, K.M. Lee, Y.S. Yoo, J.S. Yoo, J.I. Yoo, H.S. Kim, Y.S. Lee, and G.T. Chung, *Alterations of gyrA, gyrB, and parC and activity of efflux pump in fluoroquinolone-resistant* Acinetobacter baumannii, Osong. Public Health Res. Perspect. 2 (2011), pp. 164–70.

[4] J. Vila, J. Ruiz, P. Goni, A. Marcos, and T.J. De Anta, *Mutation in the gyrA gene of quinolone-resistant clinical isolates of* Acinetobacter baumannii, Antimicr. Agents Chemother. 39 (1995), pp. 1201–1203.

[5] S. Yilmaz, G. Altinkanat-Gelmez, K. Bolelli, D. Guneser-Merdan, M.U. Over-Hasdemir, I. Yildiz, E. Aki-Yalcin, and I. Yalcin, *Pharmacophore generation of 2-substituted benzothiazoles as AdeABC efflux pump inhibitors in* A. baumannii, SAR QSAR Environ. Res. 25 (2014), pp. 551–563.

[6] T. Tomasic and L.P. Masic, *Prospects for developing new antibacterials targeting bacterial type IIA topoisomerases*, Curr. Top. Med. Chem. 14 (2014), pp. 130–151.

[7] F. Collin, S. Karkare, and A. Maxwell, *Exploiting bacterial DNA gyrase as a drug target: Current state and perspectives*, Appl. Microbiol. Biotechnol. 92 (2011), pp. 479–497.

[8] M.A. Azam and J. Thathan, *Pharmacophore generation, atom-based 3D-QSAR and molecular dynamics simulation analyses of pyridine-3-carboxamide-6-yl-urea analogues as potential gyrase B inhibitors*, SAR QSAR Environ. Res. 28 (2017), pp. 275–296.

[9] J.J. Perez, C.S. Lupala, and P. Gomez-Gutierrez, *Designing type II topoisomerase inhibitors: A molecular modeling approach*, Curr. Top. Med. Chem. 14 (2014), pp. 40–50.

[10] L. Aravind, D.D. Leipe, and E.V. Koonin, *Toprim—a conserved catalytic domain in type IA and II topoisomerases*, DnaG-type primases, OLD family nucleases and RecR proteins, Nucleic Acids Res. 26 (1998), pp. 4205–4213.

[11] R. Dutta and M. Inouye, *GHKL, an emergent ATPase/kinase superfamily*, Trends Biochem. Sci. 25 (2000), pp. 24–28.
[12] G.M. Harami, M. Gyimesi, and M. Kovacs, *From keys to bulldozers: Expanding roles for winged helix domains in nucleic-acid-binding proteins*, Trends Biochem. Sci. 38 (2013), pp. 364–371.
[13] B.D. Bax, P.F. Chan, D.S. Eggleston, A. Fosberry, D.R. Gentry, F. Gorrec, I. Giordano, M.M. Hann, A. Hennessy, M. Hibbs, J. Huang, E. Jones, J. Jones, K.K. Brown, C.J. Lewis, E.W. May, M.R. Saunders, O. Singh, C.E. Spitzfaden, C. Shen, A. Shillings, A.J. Theobald, A. Wohlkonig, N.D. Pearson, and M.N. Gwynn, *Type IIA topoisomerase inhibition by a new class of antibacterial agents*, Nature 466 (2010), pp. 935–940.
[14] J.G. Heddle, S. Mitelheiser, A. Maxwell, and N.H. Thomson, *Nucleotide binding to DNA gyrase causes loss of DNA wrap*, J. Mol. Biol. 337 (2004), pp. 597–610.
[15] A.D. Bates and A. Maxwell, *Energy coupling in type II topoisomerases: Why do they hydrolyze ATP?*, Biochemistry 46 (2007), pp. 7929–7941.
[16] N.L. Williams and A. Maxwell, *Probing the two-gate mechanism of DNA gyrase using cysteine cross-linking*, Biochemistry 38 (1999), pp. 13502–13511.
[17] L.M. Oppegard, H.A. Schwanz, T.R. Towle, R.J. Kerns, and H. Hiasa, *Fluoroquinolones stimulate the DNA cleavage activity of topoisomerase IV by promoting the binding of Mg(2+) to the second metal binding site*, Biochim. Biophys. Acta 2016 (1860), pp. 569–575.
[18] B.H. Schmidt, A.B. Burgin, J.E. Deweese, N. Osheroff, and J.M. Berger, *A novel and unified two-metal mechanism for DNA cleavage by type II and IA topoisomerases*, Nature 465 (2010), pp. 641–644.
[19] S.L. Pitts, G.F. Liou, L.A. Mitchenall, A.B. Burgin, A. Maxwell, K.C. Neuman, and N. Osheroff, *Use of divalent metal ions in the DNA cleavage reaction of topoisomerase IV*, Nucleic Acids Res. 39 (2011), pp. 4808–4817.
[20] L.C. Axford, P.K. Agarwal, K.H. Anderson, L.N. Andrau, J. Atherall, S. Barker, J.M. Bennett, M. Blair, I. Collins, L.G. Czaplewski, D.T. Davies, C.T. Gannon, D. Kumar, P. Lancett, A. Logan, C.J. Lunniss, D.R. Mitchell, D.A. Offermann, J.T. Palmer, N. Palmer, G.R. Pitt, S. Pommier, D. Price, B. Narasinga Rao, R. Saxena, T. Shukla, A.K. Singh, M. Singh, A. Srivastava, C. Steele, N.R. Stokes, H.B. Thomaides-Brears, E.M. Tyndall, D. Watson, and D.J. Haydon, *Design, synthesis and biological evaluation of alpha-substituted isonipecotic acid benzothiazole analogues as potent bacterial type II topoisomerase inhibitors*, Bioorg. Med. Chem. Lett. 23 (2013), pp. 6598–6603.
[21] K. Drlica, *Mechanism of fluoroquinolone action*, Curr. Op. Microbiol. 2 (1999), pp. 504–508.
[22] I. Laponogov, M.K. Sohi, D.A. Veselkov, X.S. Pan, R. Sawhney, A.W. Thompson, K.E. McAuley, L.M. Fisher, and M.R. Sanderson, *Structural insight into the quinolone-DNA cleavage complex of type IIA topoisomerases*, Nat. Struct. Mol. Biol. 16 (2009), pp. 667–669.
[23] I. Laponogov, X.S. Pan, D.A. Veselkov, K.E. McAuley, L.M. Fisher, and M.R. Sanderson, *Structural basis of gate-DNA breakage and resealing by type II topoisomerases*, PLoS One 5 (2010), p. e11338.
[24] A. Wohlkonig, P.F. Chan, A.P. Fosberry, P. Homes, J. Huang, M. Kranz, V.R. Leydon, T.J. Miles, N.D. Pearson, R.L. Perera, A.J. Shillings, M.N. Gwynn, and B.D. Bax, *Structural basis of quinolone inhibition of type IIA topoisomerases and target-mediated resistance*, Nat. Struct. Mol. Biol. 17 (2010), pp. 1152–1153.
[25] S. Alper-Hayta, E. Aki-Sener, B. Tekiner-Gulbas, I. Yildiz, O. Temiz-Arpaci, I. Yalcin, and N. Altanlar, *Synthesis, antimicrobial activity and QSARs of new benzoxazine-3-ones*, Eur. J. Med. Chem. 41 (2006), pp. 1398–1404.
[26] *Discovery Studio 3.5, Accelrys Software Inc., San Diego* 2013; software available at http://accelrys.com/products/discoverystudio.
[27] S. Yilmaz, G. Altinkanat-Gelmez, K. Bolelli, D. Guneser-Merdan, M. Ufuk Over-Hasdemir, E. Aki-Yalcin, and I. Yalcin, *Binding site feature description of 2-substituted benzothiazoles as potential AcrAB-TolC efflux pump inhibitors in* E. coli, SAR QSAR Environ. Res. 26 (2015), pp. 853–871.
[28] I. Yalcin, B.P. Tekiner, I.Y. Oren, O.T. Arpaci, E. Aki-Sener, and N. Altanlar, *Synthesis and antimicrobial activity of some novel 2, 6, 7-trisubstituted-2H-3, 4-dihydro-1, 4-benzoxazin-3-one derivatives*, Indian J. Chem. 42B (2003), pp. 905–909.
[29] T. Kumonaka, T. Hase, T. Aotsuka, T. Kurihara, Y. Nakamura, T. Matsui, H. Ishikawa, and F. Kobayashi, *1,4-benzoxazine-2-acetic acid compound, method for production thereof and use thereof*, Google Patents, 1997.
[30] P. Barraja, P. Diana, A. Montalbano, A. Martorana, A. Carbone, and G. Cirrincione, *Synthesis of the new ring system 2-oxo-[1,4]oxazino[3,2-e]indole, heteroanalogue of Angelicin*, Tetrahedron Lett. 50 (2009), pp. 4182–4184.